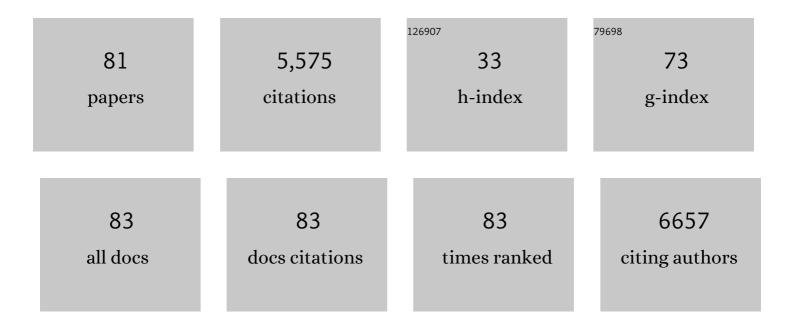
List of Publications by Year in descending order

Source: https://exaly.com/author-pdf/3907506/publications.pdf Version: 2024-02-01



WELLANC HE

#	Article	IF	CITATIONS
1	H <sub>2</sub> O <sub>2</sub> -Activatable and O <sub>2</sub> -Evolving Nanoparticles for Highly Efficient and Selective Photodynamic Therapy against Hypoxic Tumor Cells. Journal of the American Chemical Society, 2015, 137, 1539-1547.	13.7	754
2	Metal coordination in photoluminescent sensing. Chemical Society Reviews, 2013, 42, 1568.	38.1	702
3	A Ratiometric Fluorescent Probe for Rapid Detection of Hydrogen Sulfide in Mitochondria. Angewandte Chemie - International Edition, 2013, 52, 1688-1691.	13.8	491
4	Visible Light Excitable Zn <sup>2+</sup> Fluorescent Sensor Derived from an Intramolecular Charge Transfer Fluorophore and Its in Vitro and in Vivo Application. Journal of the American Chemical Society, 2009, 131, 1460-1468.	13.7	401
5	Photoluminescence imaging of Zn <sup>2+</sup> in living systems. Chemical Society Reviews, 2015, 44, 4517-4546.	38.1	225
6	Oxidative DNA Cleavage Promoted by Multinuclear Copper Complexes: Activity Dependence on the Complex Structure. Chemistry - A European Journal, 2006, 12, 6621-6629.	3.3	171
7	Ratiometric detection of pH fluctuation in mitochondria with a new fluorescein/cyanine hybrid sensor. Chemical Science, 2015, 6, 3187-3194.	7.4	165
8	An Optical/Photoacoustic Dual-Modality Probe: Ratiometric in/ex Vivo Imaging for Stimulated H <sub>2</sub> S Upregulation in Mice. Journal of the American Chemical Society, 2019, 141, 17973-17977.	13.7	156
9	Ferroptosis Photoinduced by New Cyclometalated Iridium(III) Complexes and Its Synergism with Apoptosis in Tumor Cell Inhibition. Angewandte Chemie - International Edition, 2021, 60, 8174-8181.	13.8	154
10	A Zn <sup>2+</sup> Fluorescent Sensor Derived from 2-(Pyridin-2-yl)benzoimidazole with Ratiometric Sensing Potential. Organic Letters, 2009, 11, 795-798.	4.6	118
11	A dual-labeling probe to track functional mitochondria–lysosome interactions in live cells. Nature Communications, 2020, 11, 6290.	12.8	116
12	Photoactivated Lysosomal Escape of a Monofunctional Pt <sup>II</sup> Complex Ptâ€BDPA for Nucleus Access. Angewandte Chemie - International Edition, 2019, 58, 12661-12666.	13.8	89
13	A turn-on fluorescent Fe3+ sensor derived from an anthracene-bearing bisdiene macrocycle and its intracellular imaging application. Chemical Communications, 2014, 50, 4631.	4.1	84
14	Golgi apparatus-targeted aggregation-induced emission luminogens for effective cancer photodynamic therapy. Nature Communications, 2022, 13, 2179.	12.8	83
15	A new "turn-on―chemodosimeter for Hg2+: ICT fluorophore formation via Hg2+-induced carbaldehyde recovery from 1,3-dithiane. Chemical Communications, 2012, 48, 5094.	4.1	81
16	An excitation ratiometric Zn2+ sensor with mitochondria-targetability for monitoring of mitochondrial Zn2+ release upon different stimulations. Chemical Communications, 2012, 48, 8365.	4.1	77
17	Simultaneous Zn2+ tracking in multiple organelles using super-resolution morphology-correlated organelle identification in living cells. Nature Communications, 2021, 12, 109.	12.8	71
18	A reversible ratiometric sensor for intracellular Cu2+ imaging: metal coordination-altered FRET in a dual fluorophore hybrid. Chemical Communications, 2013, 49, 7632.	4.1	68

#	Article	IF	CITATIONS
19	<i>De Novo</i> -Designed Near-Infrared Nanoaggregates for Super-Resolution Monitoring of Lysosomes in Cells, in Whole Organoids, and <i>in Vivo</i> . ACS Nano, 2019, 13, 14426-14436.	14.6	63
20	In vitro and in vivo imaging application of a 1,8-naphthalimide-derived Zn2+ fluorescent sensor with nuclear envelope penetrability. Chemical Communications, 2013, 49, 11430.	4.1	62
21	Recent advances in noble metal complex based photodynamic therapy. Chemical Science, 2022, 13, 5085-5106.	7.4	62
22	A positively charged trinuclear 3N-chelated monofunctional platinum complex with high DNA affinity and potent cytotoxicity. Dalton Transactions, 2006, , 2617.	3.3	50
23	A charge transfer type pH responsive fluorescent probe and its intracellular application. New Journal of Chemistry, 2010, 34, 656.	2.8	46
24	Nanoscale monitoring of mitochondria and lysosome interactions for drug screening and discovery. Nano Research, 2019, 12, 1009-1015.	10.4	45
25	In vivo ratiometric Zn <sup>2+</sup> imaging in zebrafish larvae using a new visible light excitable fluorescent sensor. Chemical Communications, 2014, 50, 1253-1255.	4.1	44
26	DNA Crossâ€Linking Patterns Induced by an Antitumorâ€Active Trinuclear Platinum Complex and Comparison with Its Dinuclear Analogue. Chemistry - A European Journal, 2009, 15, 5245-5253.	3.3	43
27	InÂvivo fluorescence imaging for Cu2+ in live mice by a new NIR fluorescent sensor. Dyes and Pigments, 2016, 130, 116-121.	3.7	43
28	Synergetic effect between spin crossover and luminescence in the [Fe(bpp)2][BF4]2 (bpp =) Tj ETQq0 0 0 rgBT /	Overlock 2	10 Tf 50 382 41
29	A fluorometric/colorimetric dual-channel Hg2+ sensor derived from a 4-amino-7-nitro-benzoxadiazole (ANBD) fluorophore. New Journal of Chemistry, 2011, 35, 607.	2.8	40
30	Rational construction of a reversible arylazo-based NIR probe for cycling hypoxia imaging in vivo. Nature Communications, 2021, 12, 2772.	12.8	37
31	INTERACTION OF METAL IONS WITH TWO NEW CALIX[4, 8]ARENE DERIVATIVES. Journal of Coordination Chemistry, 2001, 54, 105-116.	2.2	35
32	Synthesis and fluorescence properties of isoindoline–benzazole-based boron difluoride complexes. New Journal of Chemistry, 2014, 38, 1277.	2.8	33
33	Reversible FRET Fluorescent Probe for Ratiometric Tracking of Endogenous Fe <sup>3+</sup> in Ferroptosis. Inorganic Chemistry, 2020, 59, 10920-10927.	4.0	32
34	A dual-modal probe for NIR fluorogenic and ratiometric photoacoustic imaging of Cys/Hcy in vivo. Science China Chemistry, 2020, 63, 699-706.	8.2	32
35	A New Approach to Sensitize Antitumor Monofunctional Platinum(II) Complexes via Short Time Photo-Irradiation. Inorganic Chemistry, 2017, 56, 3754-3762.	4.0	31
36	A FRET-based fluorescent Zn <sup>2+</sup> sensor: 3D ratiometric imaging, flow cytometric tracking and cisplatin-induced Zn <sup>2+</sup> fluctuation monitoring. Chemical Science, 2020, 11, 11037-11041.	7.4	31

#	Article	IF	CITATIONS
37	In Vitro and in Vivo Fluorescent Imaging of a Monofunctional Chelated Platinum Complex Excitable Using Visible Light. Inorganic Chemistry, 2011, 50, 11847-11849.	4.0	30
38	Non-symmetric thieno[3,2- <i>b</i> ]thiophene-fused BODIPYs: synthesis, spectroscopic properties and providing a functional strategy for NIR probes. Organic Chemistry Frontiers, 2019, 6, 3961-3968.	4.5	29
39	Phosphorescence Lifetime Imaging of Labile Zn <sup>2+</sup> in Mitochondria via a Phosphorescent Iridium(III) Complex. Inorganic Chemistry, 2018, 57, 10625-10632.	4.0	28
40	Ferroptosis Photoinduced by New Cyclometalated Iridium(III) Complexes and Its Synergism with Apoptosis in Tumor Cell Inhibition. Angewandte Chemie, 2021, 133, 8255-8262.	2.0	28
41	Activity-Based Fluorescent Molecular Logic Gate Probe for Dynamic Tracking of Mitophagy Induced by Oxidative Stress. Analytical Chemistry, 2021, 93, 3502-3509.	6.5	27
42	Highly efficient FRET from aggregation-induced emission to BODIPY emission based on host–guest interaction for mimicking the light-harvesting system. RSC Advances, 2017, 7, 36021-36025.	3.6	26
43	BODIPY-derived ratiometric fluorescent sensors: pH-regulated aggregation-induced emission and imaging application in cellular acidification triggered by crystalline silica exposure. Science China Chemistry, 2018, 61, 1413-1422.	8.2	26
44	FRET-based fluorescent ratiometric probes for the rapid detection of endogenous hydrogen sulphide in living cells. Analyst, The, 2020, 145, 4233-4238.	3.5	24
45	A novel triple-mode fluorescent pH probe from monomer emission to aggregation-induced emission. RSC Advances, 2015, 5, 8912-8917.	3.6	23
46	Coumarin/BODIPY Hybridisation for Ratiometric Sensing of Intracellular Polarity Oscillation. Chemistry - A European Journal, 2018, 24, 7513-7524.	3.3	23
47	A ratiometric fluorescent probe for imaging enzyme dependent hydrogen sulfide variation in the mitochondria and in living mice. Analyst, The, 2020, 145, 5123-5127.	3.5	23
48	A new BODIPY-derived ratiometric senor with internal charge transfer (ICT) effect: colorimetric/fluorometric sensing of Ag <sup>+</sup> . Dalton Transactions, 2018, 47, 2285-2291.	3.3	21
49	A highly sensitive and selective turn-on fluorescent chemodosimeter for Cu2+ based on BODIPY and its application in bioimaging. RSC Advances, 2014, 4, 6691.	3.6	20
50	A novel luminescent lr( <scp>iii</scp> ) complex for dual mode imaging: synergistic response to hypoxia and acidity of the tumor microenvironment. Chemical Communications, 2020, 56, 8055-8058.	4.1	20
51	Structural and fluorescent study of zinc complexes of dansyl aminoquinoline. Inorganica Chimica Acta, 2007, 360, 431-438.	2.4	19
52	A mitochondria-targeting fluorescent Fe3+ probe and its application in labile Fe3+ monitoring via imaging and flow cytometry. Dyes and Pigments, 2018, 157, 328-333.	3.7	19
53	A sulfonamidoquinoline-derived Zn2+ fluorescent sensor with 1:1 Zn2+ binding stoichiometry. Inorganic Chemistry Communication, 2011, 14, 304-307.	3.9	18
54	BODIPY-based monofunctional Pt (II) complexes for specific photocytotoxicity against cancer cells. Journal of Inorganic Biochemistry, 2021, 218, 111394.	3.5	18

#	Article	IF	CITATIONS
55	A bezoimidazole-based highly selective and low-background fluorescent sensor for Zn2+. Inorganic Chemistry Communication, 2012, 15, 176-179.	3.9	17
56	Benzothiazoleâ€Pyimidineâ€Based BF <sub>2</sub> Complex for Selective Detection of Cysteine. Chemistry - an Asian Journal, 2016, 11, 202-206.	3.3	17
57	A ratiometric fluorescent sensor for tracking Cu(I) fluctuation in endoplasmic reticulum. Science China Chemistry, 2019, 62, 465-474.	8.2	17
58	DNA cleavage promoted by trigonal-bipyramidal zinc(II) and copper(II) complexes formed by asymmetric tripodal tetradendate 2-[bis(2-aminoethyl)amino]ethanol. Inorganica Chimica Acta, 2010, 363, 793-798.	2.4	16
59	A highly selective turn-on fluorescent chemodosimeter for Cr( <scp>vi</scp> ) and its application in living cell imaging. RSC Advances, 2014, 4, 2989-2992.	3.6	15
60	Zinc ions regulate opening of tight junction favouring efflux of macromolecules <i>via</i> the GSK3β/snail-mediated pathway. Metallomics, 2018, 10, 169-179.	2.4	15
61	Tuning lipophilicity for optimizing the H <sub>2</sub> S sensing performance of coumarin–merocyanine derivatives. New Journal of Chemistry, 2019, 43, 14800-14805.	2.8	15
62	Photoactivated Lysosomal Escape of a Monofunctional Pt II Complex Ptâ€BDPA for Nucleus Access. Angewandte Chemie, 2019, 131, 12791-12796.	2.0	13
63	A photoacoustic Zn2+ sensor based on a merocyanine/xanthene-6-ol hybrid chromophore and its ratiometric imaging in mice. Inorganic Chemistry Frontiers, 0, , .	6.0	13
64	Surmounting tumor resistance to metallodrugs by co-loading a metal complex and siRNA in nanoparticles. Chemical Science, 2021, 12, 4547-4556.	7.4	12
65	A PEGylated photosensitizer-core pH-responsive polymeric nanocarrier for imaging-guided combination chemotherapy and photodynamic therapy. New Journal of Chemistry, 2021, 45, 6180-6185.	2.8	12
66	Protein A Detection Based on Quantum Dots-Antibody Bioprobe Using Fluorescence Coupled Capillary Electrophoresis. International Journal of Molecular Sciences, 2014, 15, 1804-1811.	4.1	11
67	Synthesis and electrospray mass spectrometry study of Pd(II) complexes of low-rim amino acid substituted calix[4]arenes. New Journal of Chemistry, 2001, 25, 1330-1336.	2.8	10
68	Monolayer Formation of Alkyl Chain-Containing Phosphoric Acid Amphiphiles at the Air/Water (pH 5.6) Interface: Influence of Temperature and Cations. Journal of Colloid and Interface Science, 2002, 246, 335-342.	9.4	10
69	Tracking Labile Copper Fluctuation <i>In Vivo</i> / <i>Ex Vivo</i> : Design and Application of a Ratiometric Near-Infrared Fluorophore Derived from 4-Aminostyrene-Conjugated Boron Dipyrromethene. Inorganic Chemistry, 2021, 60, 18567-18574.	4.0	10
70	Synthesis, Crystal Structure, and DNAâ€Cleaving Behavior of 5‣ubstituted Benzeneâ€1,3â€bis(methylene)‣paced Dinuclear Copper(II) Complexes. Chemistry and Biodiversity, 2008, 5, 1495-1504.	2.1	9
71	Oxidative DNA cleavage promoted by polynuclear copper complexes bearing iminodiacetate chelator. Inorganica Chimica Acta, 2013, 399, 112-118.	2.4	9
72	Zinc Promotes Patient-Derived Induced Pluripotent Stem Cell Neural Differentiation via ERK-STAT Signaling. Stem Cells and Development, 2020, 29, 863-875.	2.1	9

#	Article	IF	CITATIONS
73	A new palladium complex as a dual fluorometric and colorimetric probe for rapid determination of sulfide anion. Journal of Photochemistry and Photobiology A: Chemistry, 2021, 404, 112885.	3.9	8
74	Optimizing the photodynamic therapeutic effect of BODIPY-based photosensitizers against cancer and bacterial cells. Dyes and Pigments, 2022, 202, 110255.	3.7	7
75	Title is missing!. Journal of Chemical Crystallography, 1999, 29, 1121-1125.	1.1	5
76	DNA cleavage behavior of a new p-xylyl spaced bisCu(BPA)Cl2 complex: the steric effect of a bulky p-xylyl-derived spacer. New Journal of Chemistry, 2012, 36, 644-649.	2.8	5
77	Photoinduced synergistic cytotoxicity towards cancer cells <i>via</i> Ru( <scp>ii</scp> ) complexes. Dalton Transactions, 2020, 49, 13954-13957.	3.3	5
78	Rational Design of Ratiometric Fe3+ Fluorescent Probes Based on FRET Mechanism. Chemical Research in Chinese Universities, 2022, 38, 67-74.	2.6	5
79	Recent Endeavors on Molecular Imaging for Mapping Metals in Biology. Biophysics Reports, 2020, 6, 159-178.	0.8	4
80	An Endoplasmic Reticulum-Targeted Ratiometric Fluorescent Molecule Reveals Zn2+ Micro-Dynamics During Drug-Induced Organelle Ionic Disorder. Frontiers in Pharmacology, 2022, 13, .	3.5	2
81	A novel binuclear Pd(ii) complex displaying synergic peptide cleavage behaviour. Dalton Transactions, 2020, 49, 3164-3173.	3.3	0